Chapter 16

Ketamine Induces Neuroapoptosis in Stem Cell–Derived Developing Human Neurons Possibly through Intracellular Calcium/Mitochondria/microRNA Signaling Pathway

Danielle Twaroski, Yasheng Yan, Congshan Jiang, Sarah Logan, Zeljko J. Bosnjak and Xiaowen Bai

Additional information is available at the end of the chapter

http://dx.doi.org/10.5772/intechopen.72939

Abstract

Ketamine, one of the commonly used agents in pediatric anesthesia, has been linked to neurodegeneration and cognitive dysfunction in developing animal models. Previous studies on developing neurons derived from human embryonic stem cells (hESCs) indicate that ketamine induces neuroapoptosis and the mechanisms remain largely unknown. This study aims to investigate the effect of ketamine on intracellular calcium, mitochondrial signaling, and microRNA profiles in hESCs-derived 2-week-old neurons. The neurons were exposed to ketamine for 6 or 24 hours. Neuroapoptosis was assessed by TUNEL staining. Intracellular calcium level was analyzed using Fluo-4 AM staining. The mitochondria-related neuroapoptosis pathway including mitochondrial membrane potential, cytochrome c release from mitochondria to cytosol, and mitochondrial fission was also investigated. miScript miRNA arrays were used in microRNA target identification studies. The results showed that ketamine exposure induced neuroapoptosis and alterations in intracellular calcium levels. In addition, ketamine decreased mitochondrial membrane potential, resulted in cytochrome c release from mitochondria into cytosol, and increased mitochondrial fission. Among 88 microRNAs investigated, let-7a/e, miR-21, miR-23b, miR-28-5p, and miR-423-5p were found downregulated, while miR-96 was upregulated in the neurons treated with ketamine. Collectively, our findings indicate that ketamine induces neuroapoptosis possibly through the dysregulated intracellular calcium, mitochondria, and microRNA pathway.

Keywords: ketamine, calcium, mitochondria, microRNAs, neuroapoptosis

1. Introduction

Studies performed in a variety of animal models including mice and rhesus monkeys have found that prolonged exposure of developing animals to most inhalational and intravenous anesthetic agents including sevoflurane, isoflurane, ketamine, propofol and anesthetic combinations induce neuroapoptosis [1–3]. The period of rapid synaptogenesis has been linked to the time of greatest vulnerability in developing brains to anesthetic-induced neurotoxicity [4–6]. The period of rapid brain growth in mice peaks at roughly 7 days after birth while this time frame in humans ranges from late in pregnancy until the 2nd or 3rd year of life [7, 8]. The neuroapoptosis observed in the growing brains of the young animals was also found to be coupled to long-term memory and learning deficits. For example, Shen and colleagues noted significant deficiencies in both memory and spatial learning in postnatal day 3 Sprague–Dawley rats following exposure to 1% sevoflurane. Their studies relied on the Morris water maze test to assess spatial learning/memory in the animals. Additionally, they found that these effects were both exposure number and dose dependent. They also observed that 7-week-old (adult) rats were insensitive to sevoflurane exposure with both the control and sevoflurane exposed animals displaying comparable results in the Water maze test [3]. The results of this study confirm that vulnerability to anesthetics is confined to an early period in development.

The many animal studies have raised concerns regarding the applicability of the models to humans. Of particular concern are the many rodent studies in which hemodynamic properties were not properly controlled. While extensive studies in rhesus macaques, a non-human primate model have been performed [9–14], a suitable human model in the study of anesthetic-induced neurotoxicity is currently lacking and exposure of young children to anesthetics for study purposes would be unethical. Several human epidemiologic studies have been performed and many have suggested a link between anesthetic exposure in young children and learning and behavioral abnormalities when compared to their unexposed counterparts [15–17]. However, the human epidemiologic studies face many confounding variables that are often difficult to properly account for, leaving the results of these studies uncertain. While many of these studies are still ongoing, it is imperative to develop a proper human model to assess the effects of anesthetics in young children. Our study aimed to identify an appropriate human model to assess the effects of anesthetics on the developing human brain and also to dissect out the mechanisms behind the toxicity.

Human embryonic stem cells (hESCs) are derived from the inner cell mass of a human blastocyst. In 1998 James Thompson and colleagues at the University of Wisconsin-Madison developed a technique to isolate and culture hESCs *in vitro* [18]. The formative work of this group opened up the possibility for mechanistic-based studies using a human cell line, effectively eliminating the potential concerns regarding the relevancy of studies using animal models to humans. hESCs are immature, divide indefinitely and are capable of generating cells from all three germ layers which makes these cells an ideal model of early human neurons once differentiated. Using hESC-derived neurons has provided us with a reasonable human model by which to study anesthetic-induced developmental neurotoxicity.

While many anesthetic agents are used clinically in the pediatric population, we choose to study the effects of the widely used anesthetic ketamine on our model of hESC-derived neurons. Ketamine is an N-methyl-D-aspartate-receptor antagonist and provides pain relief and sedation in children undergoing a variety of procedures. Additionally, ketamine is a drug that is often abused and abuse of ketamine during pregnancy is of concern for the developing brain of the fetus [19]. Despite the many studies implicating the negative effects of anesthetic agents on developing brains, the mechanisms behind the toxicity remain largely unknown. Possible roles of neuroinflammation, reactive oxygen species production, epigenetic changes, and calcium signaling in the mechanism of anesthetic-induced neurotoxicity have all been suggested [20–23]. However, considerable work remains to fully elucidate the mechanisms behind the neuronal toxicity. In this study, we investigated the effect of ketamine on the cell viability, intracellular calcium level, mitochondrial signaling, and microRNA profile using the hESC-derived developing human neuron model.

Proper maintenance of intracellular calcium levels is critical for nearly every cellular process. In neurons, calcium is involved in the regulation of electrical activity, cell growth, metabolic activity, and many other processes [24]. Several studies have suggested that aberrant intracellular calcium level in neurons plays a critical role in the neuronal degeneration observed in many different neurological disorders [25]. The dysregulated intracellular calcium might induce the neurotoxicity through mitochondrial signaling. Mitochondria are highly dynamic organelles that undergo continuous cycles of fusion and fission in order to maintain cellular homeostasis. Mitochondrial fusion and fission result in a change in mitochondrial shape: either elongated, tubular, interconnected mitochondrial networks, or fragmented and discontinuous mitochondria, respectively. Unbalanced fission-fusion can lead to various pathological processes including neurodegeneration [26–29]. Shifting the balance towards fission has been associated with neuronal death in age-related neurodegenerative disease and brain injury [30, 31]. Inhibition of mitochondrial fission attenuated glutamate-induced neuronal death [31], translating to an increase in cell survival in the presence of oxidative stress [32]. Recent studies from Dr. Jevtovic's groups have shown that mitochondrial fission plays an important role in anesthetic neurotoxicity. The increased mitochondrial fission was found in neonatal rat brains after a sedative dose of midazolam followed by combined nitrous oxide and isoflurane anesthesia for 6 h [33].

MicroRNAs are small, non-coding RNAs that function as negative regulators of gene expression. MicroRNAs are transcribed in hairpin structures in the nucleus by RNA polymerase II and the pri-miRNA produced is processed by the enzyme Drosha to cleave off a single hairpin loop. This forms the pre-miRNA which is exported to the cytoplasm. Once in the cytoplasm, the pre-miRNA is further processed to remove the hairpin loop and forms the mature microRNA strand. The mature microRNA strand then incorporates into an RNA-induced silencing complex where it can act to promote silencing of its target genes [34, 35]. Over 1000 microRNAs have been discovered in humans and they have been shown to play an important role in nearly every cellular process. Dysregulation of microRNAs has also been linked to several diseases including certain cancers [36]. The role of microRNAs in anesthetic-induced neurotoxicity is just beginning to be studied.

This chapter will outline: (1) the use of hESCs as a model system to study anesthetic-induced neurotoxicity in the developing human brain, (2) the protocols involved in dissecting the mechanisms behind anesthetic-induced developmental neurotoxicity. We have focused on the role of deregulated intracellular calcium, mitochondrial signaling (e.g., mitochondrial membrane potential, cytochrome c release from mitochondria into cytosol, and mitochondrial fission), and microRNAs, and (3) a brief discussion on the possible role of intracellular calcium levels, mitochondrial signaling, and altered microRNA profiles in ketamine-induced developmental neurotoxicity.

2. Materials and methods

2.1. Stem cell culture and neuronal differentiation

hESCs (H1 cell line, WiCell Research Institute Inc., Madison, WI) were cultured on a feeder layer of mouse embryonic fibroblasts (MEFs) that were mitotically inactivated using mitomycin C (Sigma-Aldrich, St. Louis, MO) in hESC media containing DMEM/F12 supplemented with, 1% nonessential amino acids, 20% Knockout serum (Gibco), 1 mM L-glutamine, 4 ng/mL human recombinant basic fibroblast growth factor (bFGF, Invitrogen), 1% penicillin–streptomycin (Invitrogen) and 0.1 mM β-mercaptoethanol (Sigma-Aldrich). The media was changed daily and the cells were mechanically passaged every 5–6 days. For the studies described in this chapter, hESCs at passage 55–70 were used. To generate neurons, the hESCs were taken through a four-step differentiation protocol. The hESCs were dissociated using the protease Dispase (1.5 unit/mL, Invitrogen). The hESCs were then cultured in ultra-low attachment six-well plates (Corning Inc., Corning, NY) in a normoxic incubator (20% O_2/5% CO_2, 37°C). The media was changed once per day and spherical embryoid bodies (EBs) were present 24 h after dispase digestion. Five days after digestion, EBs were moved to neural induction media containing DMEM/F12 supplemented with 1% N_2 (Invitrogen), 1% nonessential amino acids, 1 mg/mL heparin (Sigma) and 5 ng/mL bFGF. On day 9, the EBs were plated to matrigel-coated 35-mm dishes. Rosette-like structures were present within 5 days of the EBs plating down. The rosettes were manually separated from the surrounding cells using a serological pipette approximately 2 days after the morphology was clearly visible. The rosette cells were then transferred to matrigel-coated culture dishes and cultured in neural expansion media containing DMEM/F12 supplemented with 2% B27 without vitamin A, 1% N_2 (Invitrogen), 1% nonessential amino acids, 20 ng/mL bFGF and 1 mg/mL heparin. The neural stem cells (NSCs) were passaged enzymatically every 5 days. NSCs were cultured in 60-mm matrigel-coated dishes (500,000 cells/dish) in neuron differentiation media containing neurobasal media (Gibco) supplemented with 2% B27, 100 ng/mL ascorbic acid (Sigma-Aldrich), 0.1 μM cyclic adenosine monophosphate, 10 ng/mL brain-derived neurotrophic factor, 10 ng/mL insulin-like growth factor 1 (PeproTech Inc., Rocky Hill, NJ) and 10 ng/mL glial cell-derived neurotrophic factor. The media was changed every other day. Following 2 weeks of culture, the cells displayed clear neuronal morphology and were used for the studies.

2.2. Neuronal characterization by immunofluorescence staining

hESC-derived neurons cultured on matrigel-coated, glass coverslips for 2 weeks were fixed for 30 min in 1% paraformaldehyde at room temperature. The cells were then washed with phosphate-buffered saline (PBS). Next, the cells were incubated for 15 min in 0.5% Triton X-100 (Sigma-Aldrich) in PBS. The cells were washed once again with PBS and blocked for 20 min with 10% donkey serum at room temperature. The cells were then incubated with the primary antibodies [microtubule-associated protein 2 (MAP2), β-tubulin III or doublecortin (Abcam, Cambridge, MA)] for 1 h in a humidified, 37°C incubator. The cells were washed with PBS and incubated for 45 min with Alexa Fluor 488 or 594 donkey anti-mouse or rabbit immunoglobulin G (Invitrogen) secondary antibodies at 37°C. The cell nuclei were stained with Hoechst 33342 (Invitrogen). The coverslips were then mounted onto glass slides and imaged using a laser-scanning confocal microscope (Nikon Eclipse TE2000-U, Nikon Inc., Melville, NY).

2.3. Ketamine exposure

While the brain concentration of ketamine in humans during the induction and maintenance of anesthesia is not well understood, reports have found that the peak blood levels of ketamine could be as high as 103 μM. The levels required to maintain anesthesia are typically in the range of 10–20 μM. hESC-derived neurons were exposed to 6 h of 20 μM ketamine or neurobasal media as a vehicle-control in a 5% CO_2 incubator with normoxic conditions only for the microRNA studies. For all remaining studies, the cells were exposed to 24 h of 20 or 100 μM ketamine or neurobasal media as the vehicle control in the same incubator.

2.4. Assessment of cell death by TUNEL staining

Apoptosis of the hESC-derived neurons was assessed using a cell death detection kit (Roche Applied Bio Sciences, Indianapolis, IN) based on terminal deoxynucleotidyl transferase-mediated deoxyuridine triphosphate in situ nick end labeling (TUNEL) following directions provided by the manufacturer. This kit identifies single or double-stranded DNA breaks by labeling the free 3′-OH termini with altered nucleotides in a reaction with terminal deoxynucleotidyl transferase (TdT). Cells cultured on glass coverslips were exposed to ketamine or control conditions, rinsed and fixed with 1% paraformaldehyde. DNA fragmentation was analyzed using TdT, which incorporates into sites of DNA breaks. The nuclei were stained with Hoechst 33342 and the cells were imaged using the confocal microscope. Apoptosis/necrosis was quantified by assessing the ratio of TUNEL-positive nuclei to total cell nuclei in a field.

2.5. Calcium imaging

Neurons were plated on matrigel-coated glass coverslips for the calcium imaging studies. Intracellular calcium was assayed using Fluo-4AM (Thermo Fisher Scientific). Neurons were

loaded with 2 μM Fluo-4AM for 30 min in the presence/absence of ketamine at 37°C followed by a 20-min washout deesterification. The coverslips were placed in a polycarbonate recording chamber (Warner Instruments) on the stage of a laser-scanning confocal microscope. Fluo-4AM fluorescence ($\lambda_{ex}/\lambda_{em}$ = 485/520 nm) was visualized using the confocal microscope and the studies were completed in under 8 min to ensure minimal confounding stress to the cells. Fluorescent intensity was then quantified using ImageJ software 1.41 (Wayne Rasband; National Institutes of Health).

2.6. Mitochondrial membrane potential ($\Delta\Psi_m$) assay

hESC-derived neurons cultured on glass coverslips were incubated with 50 nM tetramethylrhodamine ethyl ester (TMRE) (Thermo Fisher Scientific) for 20 min at room temperature. TMRE fluorescent intensity representing $\Delta\Psi_m$ was recorded using the confocal microscope (Nikon). Images were obtained from six random fields per coverslip. The data were analyzed using ImageJ software.

2.7. Analysis of release of cytochrome c from mitochondria into cytosol

NSCs were cultured in neuronal differentiation medium. Ten days later, the differentiated neurons were transduced with the virus CellLight™ mitochondria-green fluorescence protein (GFP) (Thermo Fisher Scientific) for 24 h to label mitochondria. This fluorescent protein-based reagent contains the leader sequence of E1-α pyruvate dehydrogenase fused to emerald GFP. The transduced neurons expressed GFP within mitochondria. Four days later, the labeled neurons were used for analysis of the effect of ketamine on the cytochrome c translocation. Virus transduction efficiency was calculated as the ratio between GFP-positive cells and total cells. GFP expression in mitochondria was confirmed by the colocalization of GFP and TMRE fluorescence signals within cells. The distribution of cytochrome c in the neurons was analyzed using immunofluorescence staining with antibody against cytochrome c (Abcam).

2.8. Assessment of mitochondrial shape by electron microscopy

hESC-derived neurons were cultured on matrigel-coated plastic coverslips and were exposed to either 20 μM or 100 μM ketamine or control conditions for 24 h. The cells were fixed at 4°C with 2% glutaraldehyde in 0.1 M sodium cacodylate buffer and postfixed for 1 h on ice with 1% osmium tetroxide. The cells were rinsed with distilled water and dehydrated using acetonitrile and graded methanol (50%, 20 min; 70%, 20 min; 95%, 20 min; 100% 3×, 20 min). The cells were embedded in epoxy resin (EMbed-812, Electron Microscopy Sciences, Hatfield, PA) and polymerized at 70°C overnight. Thin (60 nm) sections were cut and the sections were stained with lead citrate and uranyl acetate. The samples were imaged using a Hitachi H600 Electron Microscope.

2.9. RNA extraction and cDNA preparation

Following exposure to ketamine or control conditions, total RNA was extracted using an RNeasy mini kit (Qiagen, Valencia, CA). Briefly, the cells were rinsed with PBS and lysed with QIAzol lysis reagent (Qiagen). Chloroform was added and the lysates were centrifuged. The upper phase was

removed and RNA was precipitated from it with 100% ethanol. The RNA was collected using the RNeasy spin columns (Qiagen). The samples were rinsed with buffer RPE. To elute the RNA from the column, 30 μL of RNase-free water (Qiagen) was added. An Epoch nanodrop spectrophotometer (BioTek Instruments Inc., Winooski, VT) was used to assess the quantity and quality of the RNA in each sample. Each RNA sample was then diluted to 100 ng/μL in RNase-free water. The RNA was reverse transcribed to cDNA using the miScript II RT kit (Qiagen) following the manufacturer's directions. Briefly, a mixture containing 1 μg of RNA, RNase-free water, 10× miScript nucleics mix, reverse transcriptase mix and 5× HiSpec buffer (Qiagen) was prepared. The RT reaction mixture was incubated for 1 h at 37°C and for 5 min at 95°C to stop the reaction. The RT product was diluted in 200 μL in RNase-free water which yielded a final RNA concentration of 4.5 ng/μL in each sample.

2.10. Quantitative reverse transcription-PCR (qRT-PCR) analysis of MicroRNAs

To screen for potential microRNAs contributing to the ketamine-induced neurotoxicity, we used human miFinder miRNA PCR arrays (Qiagen) which screen 84 microRNAs. For the arrays, a master mix (25 μL/well) containing the template cDNA (4.5 ng/well), RNase-free water, universal primer and miScript SYBR Green (Qiagen) was prepared according to the manufacturer's instructions. The primers for each microRNAs to be analyzed come lyophilized in the wells of the array plates. To confirm the array results, validation assays were performed in which the three cDNA samples used for the arrays were each run in triplicate on the same PCR run. The PCR was run using a BioRad iCycler for 15 min at 95°C followed by 40 cycles of: denaturation (15 s at 94°C), annealing (30 s at 55°C) and extension (30 s at 70°C). Melt curve and reverse transcriptase controls were run to ensure sample purity and primer specificity, respectively. The epoch nanodrop spectrophotometer was also used to assess RNA quality using the A260:A280 ratio. To be considered pure, the A260:A280 for an RNA sample must fall between 1.8 and 2.2. Samples with an A260:A280 ratio outside of this accepted range were not used for the studies. MicroRNAs that displayed a 1.3 fold change in expression between the ketamine and control treated cells were considered to be of interest.

2.11. Statistical analysis

The data presented in this chapter was all collected from at least 3 independent neuronal differentiations. Values were reported as means ± the standard deviation with normal distributions. Statistical analysis was completed using the Student's t-test when comparing 2 groups. All statistical analysis was performed using the SigmaStat 3.5 software (Systat Software, Inc., San Jose, CA).

3. Results and discussion

3.1. Neuronal differentiation and characterization

To generate neurons from the hESCs, the cells were taken through a four-step differentiation protocol as outlined in **Figure 1A** and described previously [20, 37, 38]. The neurons

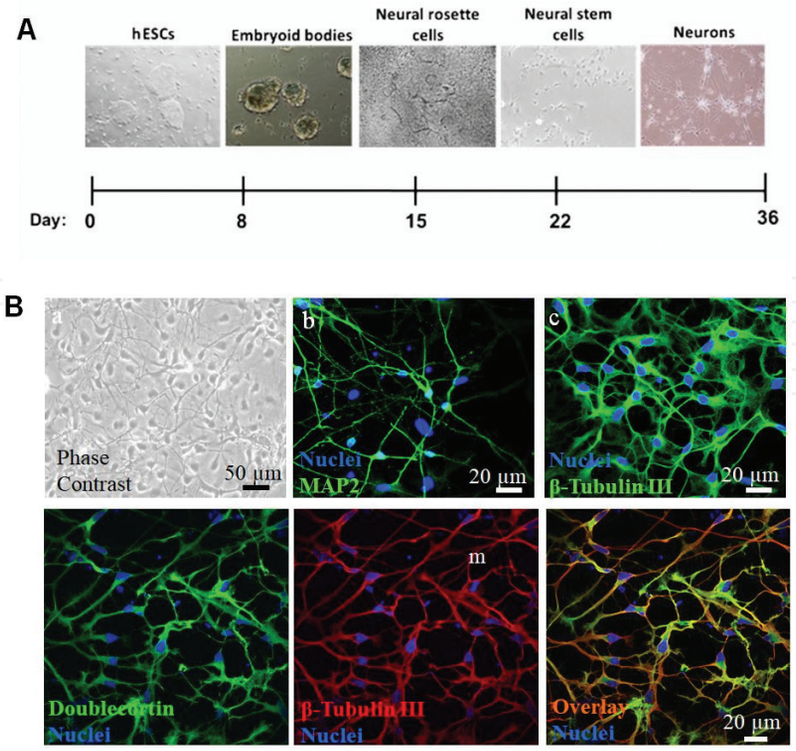

Figure 1. Differentiation protocol and confocal images of immunolabeled human embryonic stem cell (hESC)-derived neurons. (A) Neurons were derived from hESCs through a four step differentiation protocol. (B) Neurons were stained with antibodies against the neuron-specific proteins, microtubule-associated protein 2 (MAP2) and β-tubulin III to assess the differentiation efficiency, and doublecortin to confirm the immaturity of the neurons [37].

exhibited a characteristic neuronal morphology with small cell bodies and long projections. The neurons also formed extensive, interconnected networks over time. The cells displayed a very distinct morphology at each stage of the differentiation protocol. The hESCs formed tight colonies when cultured on a feeder layer and the EBs formed three-dimensional aggregates when suspended in culture media. At the neural rosette stage, the NSCs formed tightly packed arrangements with a characteristic design and were bordered by several additional cell types. Once mechanically separated from the surrounding non-NSCs and digested, the NSCs separated from one another and spread out on the matrigel-coated dishes. At this point, the cells proliferated extensively.

The neurons were immunostained after 2 weeks in differentiation media and expressed the neuron-specific markers MAP2 and β-tubulin III and formed synapses as assessed by the positive staining of Synapsin I. Based upon the immunostaining, the differentiation protocol was 90–95% efficient in the generation of neurons. In an attempt to better gauge the maturity level of the hESC-derived neurons, the cells were also immunostained for doublecortin, a marker of immature/migrating neurons. In assessing the staining results, most of the neurons in culture (90–95%) were positive for this marker of immature neurons (**Figure 1B**) which suggests that this model system is a valuable representation of developing human neurons.

3.2. Ketamine-induced apoptosis

TUNEL staining was used to assess cell death in hESC-derived neurons following ketamine exposure by labeling breaks in the DNA. The cells were exposed to 100 μM ketamine or control conditions for 24 h. The number of TUNEL-positive cells was significantly increased when compared to control treated cells following ketamine exposure (**Figure 2**). These findings confirm many of the previously published animal studies which have shown increased neuronal cell death following exposure of the developing brain to ketamine [39]. We focused on the investigation of the effect of ketamine on the intracellular calcium level, mitochondrial signaling, and microRNA expression in order to understand the mechanisms governing ketamine-induced cell death.

3.3. Alterations in intracellular calcium levels

Following exposure of 2-week-old hESC-derived neurons to 100 μM ketamine or control conditions for 24 h, the intracellular calcium levels in the cells were assessed using Fluo-4AM fluorescence. The intracellular calcium levels were significantly elevated in the ketamine-treated cells when compared to control treatment (**Figure 3**). Calcium is a critical ion in the body and is fundamental in proper neuronal functioning. In neurons, calcium is crucial in synaptic activity and plasticity, cell signaling, neurotransmitter release and is involved in nearly every aspect of the cell cycle [24]. The careful balance of intracellular calcium levels is crucial to cell survival. Calcium homeostasis dysregulation, in particular calcium overload in the cell, has been linked to many different neurodegenerative diseases [25]. The findings from this study suggest that disrupted intracellular calcium homeostasis may also be linked to ketamine-induced cell death in developing neurons which could prove to be a novel therapeutic target.

3.4. Ketamine induces neuronal apoptosis via mitochondrial pathway

The mitochondria are extremely important organelles involved in many cellular processes including energy production, cell signaling, and apoptosis [40–46]. Given that ketamine may

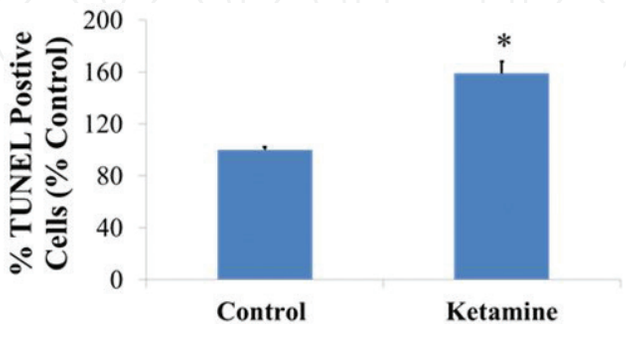

Figure 2. Exposure to 100 μM ketamine for 24 h induced significant cell death in the hESC-derived neurons. Ketamine induced an increase in the number of TUNEL-positive cells indicating significant cell death when compared to control-treated cells. *P < 0.05 vs. control. n = 3 for each group.

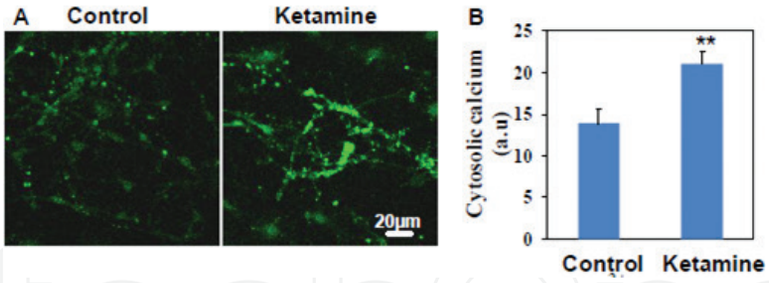

Figure 3. Ketamine exposure for 24 h induced elevated cytosolic Ca^{2+} [$(Ca^{2+})_c$] of neurons. (A) Ketamine increased $(Ca^{2+})_c$. Neurons were loaded with the Ca^{2+} indicator Fluo-4AM. The fluorescence images of free cytosolic Ca^{2+} in the 2-week-old differentiated neurons are shown. (B) Ketamine (100 μM, 24 h) significantly increased $(Ca^{2+})_c$ (**$P < 0.01$, $n = 3$).

cause mitochondrial damage, we measured $\Delta\Psi_m$ and distribution of cytochrome c in the cells. Treatment of hESC-derived neurons with 100 μM ketamine for 24 h significantly decreased $\Delta\Psi_m$ (**Figure 4A**). In order to investigate the distribution of cytochrome c within the cells, the neurons were transduced with the virus CellLight™ mitochondria-GFP (green). GFP and TMRE signals were colocalized in the cells (**Figure 4B**), confirming that successfully labeling of mitochondria with GFP. GFP-positive cells reached 40% (**Figure 4C**). The distribution of cytochrome c in mitochondria and cytosol was examined using immunofluorescence staining. The results showed that cytochrome c was located within mitochondria in the control culture (**Figure 4D**). However, in the ketamine-treated cells, cytochrome c was released from the mitochondria into cytosol.

Neuroapoptosis is a commonly recognized harmful effect by anesthetics with mechanisms that are not fully understood. Apoptosis is a programmed cell death. Cytochrome c release from mitochondria precededing the loss of $\Delta\Psi_m$ is a key event in initiating mitochondria-involved apoptosis [47], eventually leading to the typical alterations related to apoptosis such as DNA fragmentation in cell nuclei [48, 49]. In this study, following ketamine exposure, there was a significantly increase in the TUNEL-positive apoptotic cells (**Figure 2**). Ketamine-induced cell death was accompanied by the significant decrease in $\Delta\Psi_m$ and the increased cytochrome c release from mitochondria into cytosol (**Figure 4**). These data were in agreement with those previously reported by others [48, 50–52], suggesting that ketamine induces human neuron to undergo mitochondria-mediated apoptosis pathway.

To maintain proper cellular function, the mitochondria continuously undergo cycles of fusion and fission. Unbalanced fusion/fission, particularly excessive fission/fragmentation can lead to various pathological conditions including neurodegeneration [53]. To assess mitochondrial fission shape in the hESC-derived neurons following exposure to ketamine, electron microscopy was used. The neurons were exposed to either 20 μM or 100 μM ketamine or control conditions for 24 h. The cells were then prepared and imaged on an electron microscope. The mitochondria appeared considerably fragmented in the ketamine- treated neurons when compared to control cells (**Figure 5**). Increased mitochondrial fission has been linked to the propofol-induced cell death in hESC-derived neurons as previously published by our group [54]. Our findings suggest that ketamine exposure results in an increase of mitochondrial fission within the developing neurons, which may contribute to the increased cell death observed in the ketamine-treated group.

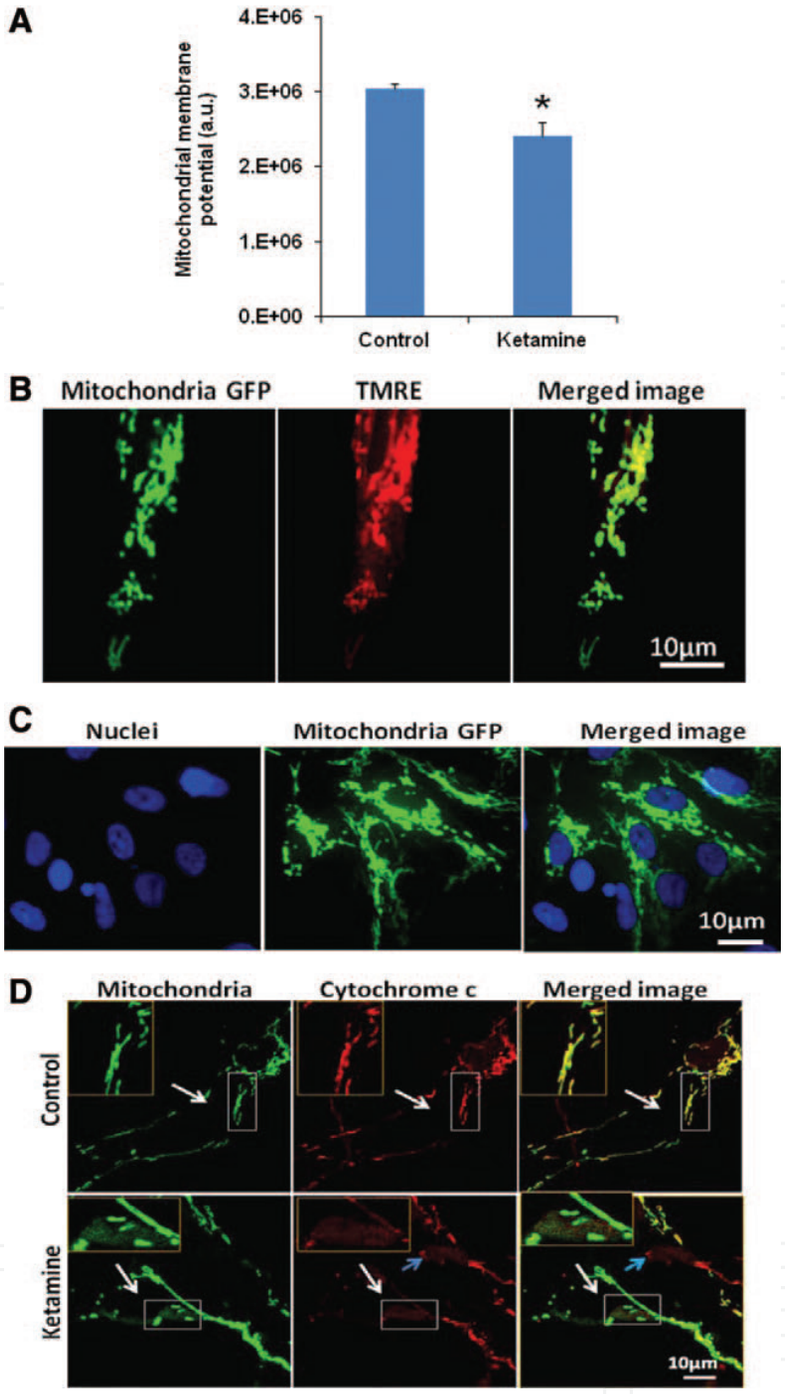

Figure 4. Ketamine decreases mitochondrial membrane potential ($\Delta\Psi_m$) and increases cytochrome c release from mitochondria into cytosol. (A) $\Delta\Psi_m$ assay. Ketamine (100 Mm) treatment for 24 h decreased $\Delta\Psi_m$ (*$P < 0.05$ vs. control, $n = 3$). (B) Labeling mitochondria of neurons with CellLight™ mitochondria-green fluorescence protein (GFP) reagent. The GFP-positive cells were loaded with TMRE. GFP expression in mitochondria was confirmed by the colocalization of tetramethylrhodamine ethyl ester (TMRE/mitochondrial probe) and GFP signals within the cells. (C) Representative fluorescent images of the neurons transduced with CellLight™ mitochondria-GFP reagent. Blue are cell nuclei. 40% cells were GFP positive. (D) the effect of ketamine on the distribution of cytochrome c in neurons. Cells were labeled with CellLight™ mitochondria-GFP reagent expressed GFP in mitochondria and then treated with ketamine (100 μM, 24 h). The distribution of cytochrome c in cells was analyzed by immunofluorescence staining. Column 1 is the image of mitochondria; column 2 is the image of cytochrome c; and column 3 is the merged image. The inset in the top corner of each image is the magnified box indicated by white arrows. The orange signals in the merged images indicate the existence of cytochrome c inside the mitochondria, and the signals in the merged images indicate the existence of cytochrome c outside the mitochondria. Ketamine treatment (100 μM, 24 h) increased cytochrome c release from mitochondria into cytosol. *Note: The cytochrome c signals (indicated by blue arrows) that do not overlap with GFP florescence were from non-transduced cells*. Scale bar = 10 μm [20].

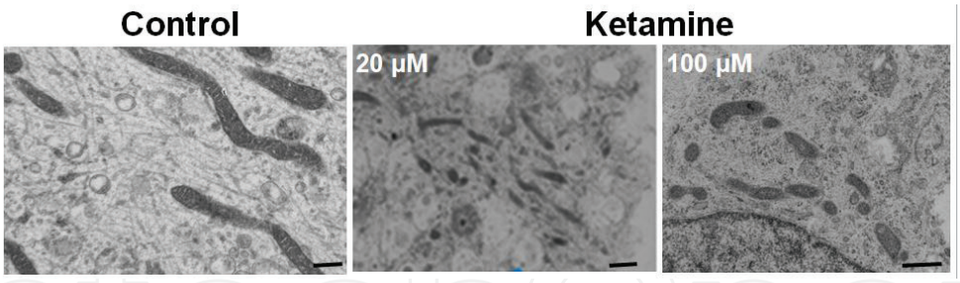

Figure 5. Ketamine increases mitochondrial fission as evidenced by the electron microscope images of differentiated neurons treated with the indicated concentrations (20 and 100 μM) of ketamine for 24 h. Scale bars = 500 nm.

3.5. qRT-PCR analysis of microRNA expression

Our lab was the first to show the role of microRNAs, specifically miR-21 in propofol-induced neurotoxicity in hESC-derived neurons [37]. Using a similar approach, we have identified several microRNAs with altered expression profiles in ketamine-treated hESC-derived neurons when compared to control-treated cells suggesting a role of microRNAs in ketamine-induced neurotoxicity. A total of 84 of the most abundantly expressed microRNAs were analyzed using the miFinder miRNA PCR arrays. A fold change of 1.3 between the control and ketamine-treated cells was considered significant. The data are expressed as percent of control with the control group set to 100%. The expression of seven microRNAs was found to be significantly altered following exposure to 6 h of ketamine when compared to control-treated cells. Of these seven, only miR-96 was found to be significantly upregulated with ketamine treatment. The remaining microRNAs (miRs-Let 7A, Let 7E, 21, 23b, 28-5p, 423-5p) were significantly downregulated with ketamine exposure compared to control-treated cells (**Figure 6**). Of these microRNAs, the downregulation of miR-21 was of particular interest since miR-21 is protective against ischemic injuries [55]. Downregulation of a protective microRNA may provide a mechanism by which ketamine is inducing neuronal toxicity in the hESC-derived neurons. Interestingly, we also reported a significant downregulation of miR-21 in hESC-derived neurons following exposure to the anesthetic propofol and went on to confirm a functional role of this expression change in the propofol-induced neurotoxicity [37]. This research suggests that the mechanism of anesthetic-induced neurotoxicity among multiple anesthetic agents might converge on altered expression of microRNAs such as miR-21. While the other 6 microRNAs identified through these array studies have not been implicated previously in neuronal diseases, this approach has the potential to uncover novel roles of these microRNAs in ketamine-induced neurotoxicity. An aim of future studies will include functional studies to further elucidate the role of these microRNAs and the signaling components connecting these altered microRNAs and attenuated mitochondrial function in ketamine-induced neurotoxicity. Additionally, the current microRNA studies were done using a different time point (6 h) than the cell death and mitochondrial studies previously mentioned which used a time point of 24 h. This was done to ensure any potentially transient changes in microRNA expression were observed. Future studies will include the addition of microRNA

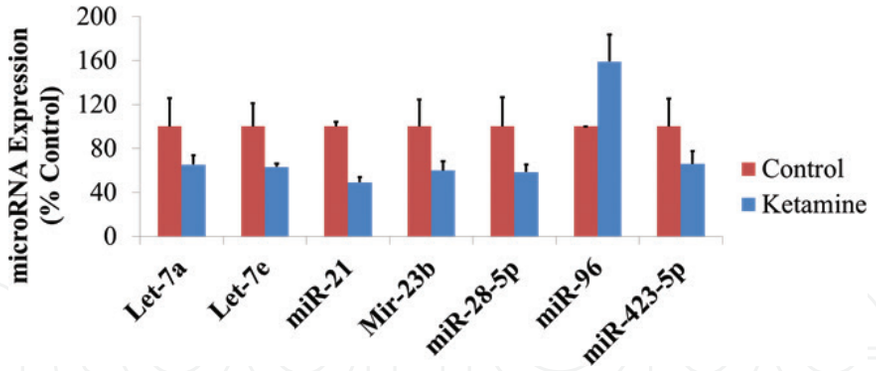

Figure 6. The expression of several microRNAs was significantly altered following exposure to ketamine. Among 88 microRNAs investigated, exposure to ketamine decreased the expression of six microRNAs and increased the expression of one microRNA. n = 3–4 for each group.

expression changes following exposure to 24 h of ketamine along with additional cell death and mitochondrial signaling assays following 6 h of exposure to ketamine which will allow for proper interpretation of the results.

3.6. Summary

The mechanisms governing anesthetic-induced neurotoxicity in the developing brain are currently not well understood and this research has been limited by the lack of an appropriate human model. Collectively, the findings from this study indicate that (1) hESC-derived neurons represent a promising model to investigate the effects of anesthetic exposure in the developing human brain, (2) ketamine induces neuroapoptosis via mitochondrial pathway, and (3) dysregulation of intracellular calcium, increased mitochondrial fission, and altered microRNA expression might play important roles in ketamine-induced neuroapoptosis. The role of microRNAs in anesthetic-induced neurotoxicity is just beginning to be understood. Functional studies including knockdown and overexpression of microRNAs of interest will further establish their role in the ketamine-induced neurotoxicity. Additionally, much work remains to establish a functional link between dysregulation of intracellular calcium, increased mitochondrial fission, decreased mitochondrial membrane potential, altered microRNA expression, and the observed neuroapoptosis. These studies are very promising and may reveal novel mechanisms of ketamine-induced developmental neurotoxicity.

Acknowledgements

The following grants supported this work: R01GM112696 from the NIH (to Dr. Xiaowen Bai) and P01GM066730 from the NIH (to Dr. Zeljko J. Bosnjak).

Author details

Danielle Twaroski[2], Yasheng Yan[1], Congshan Jiang[1], Sarah Logan[2], Zeljko J. Bosnjak[1,2] and Xiaowen Bai[1,2]*

*Address all correspondence to: xibai@mcw.edu

1 Department of Anesthesiology, Medical College of Wisconsin, Milwaukee, WI, United States

2 Department of Physiology, Medical College of Wisconsin, Milwaukee, WI, United States

References

[1] Jevtovic-Todorovic V, Hartman RE, Izumi Y, Benshoff ND, Dikranian K, Zorumski CF, Olney JW, Wozniak DF. Early exposure to common anesthetic agents causes widespread neurodegeneration in the developing rat brain and persistent learning deficits. The Journal of Neuroscience. 2003;**23**(3):876-882. PubMed PMID: 12574416

[2] Kahraman S, Zup SL, McCarthy MM, Fiskum G. GABAergic mechanism of propofol toxicity in immature neurons. Journal of Neurosurgical Anesthesiology. 2008;**20**(4):233-240. DOI: 10.1097/ANA.0b013e31817ec34d. PubMed PMID: 18812886; PMCID: PMC2730603

[3] Shen X, Liu Y, Xu S, Zhao Q, Guo X, Shen R, Wang F. Early life exposure to sevoflurane impairs adulthood spatial memory in the rat. Neurotoxicology. 2013;**39**:45-56. DOI: 10.1016/j.neuro.2013.08.007. PubMed PMID: 23994303

[4] Jevtovic-Todorovic V. Developmental synaptogenesis and general anesthesia: A kiss of death? Current Pharmaceutical Design. 2012;**18**(38):6225-6231. PubMed PMID: 22762476

[5] Jevtovic-Todorovic V. General anesthetics and the developing brain: Friends or foes? Journal of Neurosurgical Anesthesiology. 2005;**17**(4):204-206. PubMed PMID: 16184065

[6] Lunardi N, Ori C, Erisir A, Jevtovic-Todorovic V. General anesthesia causes long-lasting disturbances in the ultrastructural properties of developing synapses in young rats. Neurotoxicity Research. 2010;**17**(2):179-188. DOI: 10.1007/s12640-009-9088-z. PubMed PMID: 19626389; PMCID: PMC3629551

[7] Dobbing J, Sands J. Comparative aspects of the brain growth spurt. Early Human Development. 1979;**3**(1):79-83. PubMed PMID: 118862

[8] Dekaban AS. Changes in brain weights during the span of human life: Relation of brain weights to body heights and body weights. Annals of Neurology. 1978;**4**(4):345-356. DOI: 10.1002/ana.410040410. PubMed PMID: 727739

[9] Brambrink AM, Evers AS, Avidan MS, Farber NB, Smith DJ, Martin LD, Dissen GA, Creeley CE, Olney JW. Ketamine-induced neuroapoptosis in the fetal and neonatal rhesus macaque brain. Anesthesiology. 2012;**116**(2):372-384. DOI: 10.1097/ALN.0b013e318242b2cd. PubMed PMID: 22222480; PMCID: PMC3433282

[10] Brambrink AM, Evers AS, Avidan MS, Farber NB, Smith DJ, Zhang X, Dissen GA, Creeley CE, Olney JW. Isoflurane-induced neuroapoptosis in the neonatal rhesus macaque brain. Anesthesiology. 2010;**112**(4):834-841. DOI: 10.1097/ALN.0b013e3181d049cd. PubMed PMID: 20234312; PMCID: PMC3962067

[11] Creeley C, Dikranian K, Dissen G, Martin L, Olney J, Brambrink A. Propofol-induced apoptosis of neurones and oligodendrocytes in fetal and neonatal rhesus macaque brain. British Journal of Anaesthesia. 2013;**110**(Suppl 1):i29-i38. DOI: 10.1093/bja/aet173. PubMed PMID: 23722059; PMCID: PMC3667347

[12] Paule MG, Li M, Allen RR, Liu F, Zou X, Hotchkiss C, Hanig JP, Patterson TA, Slikker W Jr, Wang C. Ketamine anesthesia during the first week of life can cause long-lasting cognitive deficits in rhesus monkeys. Neurotoxicology and Teratology. 2011;**33**(2):220-230. DOI: 10.1016/j.ntt.2011.01.001. PubMed PMID: 21241795; PMCID: PMC3071878

[13] Slikker W Jr, Zou X, Hotchkiss CE, Divine RL, Sadovova N, Twaddle NC, Doerge DR, Scallet AC, Patterson TA, Hanig JP, Paule MG, Wang C. Ketamine-induced neuronal cell death in the perinatal rhesus monkey. Toxicological Sciences. 2007;**98**(1):145-158. DOI: 10.1093/toxsci/kfm084. PubMed PMID: 17426105

[14] Zou X, Patterson TA, Divine RL, Sadovova N, Zhang X, Hanig JP, Paule MG, Slikker W, Jr., Wang C. Prolonged exposure to ketamine increases neurodegeneration in the developing monkey brain. International Journal of Developmental Neuroscience 2009;**27**(7): 727-731. DOI: 10.1016/j.ijdevneu.2009.06.010. PubMed PMID: 19580862

[15] DiMaggio C, Sun LS, Kakavouli A, Byrne MW, Li GA. Retrospective cohort study of the association of anesthesia and hernia repair surgery with behavioral and developmental disorders in young children. Journal of Neurosurgical Anesthesiology. 2009;**21**(4):286-291. DOI: 10.1097/ANA.0b013e3181a71f11. PubMed PMID: 19955889; PMCID: PMC2789336

[16] Wilder RT, Flick RP, Sprung J, Katusic SK, Barbaresi WJ, Mickelson C, Gleich SJ, Schroeder DR, Weaver AL, Warner DO. Early exposure to anesthesia and learning disabilities in a population-based birth cohort. Anesthesiology. 2009;**110**(4):796-804. DOI: 10.1097/01.anes.0000344728.34332.5d. PubMed PMID: 19293700; PMCID: PMC2729550

[17] Ing C, DiMaggio C, Whitehouse A, Hegarty MK, Brady J, von Ungern-Sternberg BS, Davidson A, Wood AJ, Li G, Sun LS. Long-term differences in language and cognitive function after childhood exposure to anesthesia. Pediatrics. 2012;**130**(3):e476-e485. DOI: 10.1542/peds.2011-3822. PubMed PMID: 22908104

[18] Thomson JA, Itskovitz-Eldor J, Shapiro SS, Waknitz MA, Swiergiel JJ, Marshall VS, Jones JM. Embryonic stem cell lines derived from human blastocysts. Science. 1998;**282**(5391): 1145-1147. PubMed PMID: 9804556

[19] Zhao T, Li C, Wei W, Zhang H, Ma D, Song X, Zhou L. Prenatal ketamine exposure causes abnormal development of prefrontal cortex in rat. Scientific Reports. 2016;**6**:26865. DOI: 10.1038/srep26865. PubMed PMID: 27226073; PMCID: PMC4881038

[20] Bai X, Yan Y, Canfield S, Muravyeva MY, Kikuchi C, Zaja I, Corbett JA, Bosnjak ZJ. Ketamine enhances human neural stem cell proliferation and induces neuronal apoptosis

via reactive oxygen species-mediated mitochondrial pathway. Anesthesia and Analgesia. 2013;**116**(4):869-880. DOI: 10.1213/ANE.0b013e3182860fc9. PubMed PMID: 23460563; PMCID: PMC3606677

[21] Han XD, Li M, Zhang XG, Xue ZG, Cang J. Single sevoflurane exposure increases methyl-CpG island binding protein 2 phosphorylation in the hippocampus of developing mice. Molecular Medicine Reports. 2015;**11**(1):226-230. DOI: 10.3892/mmr.2014.2751. PubMed PMID: 25338822

[22] Cui Y, Ling-Shan G, Yi L, Xing-Qi W, Xue-Mei Z, Xiao-Xing Y. Repeated administration of propofol upregulated the expression of c-Fos and cleaved-caspase-3 proteins in the developing mouse brain. Indian J Pharmacol. 2011;**43**(6):648-651. DOI: 10.4103/0253-7613.89819. PubMed PMID: 22144767; PMCID: PMC3229778

[23] Wei H. The role of calcium dysregulation in anesthetic-mediated neurotoxicity. Anesthesia and Analgesia. 2011;**113**(5):972-974. DOI: 10.1213/ANE.0b013e3182323261. PubMed PMID: 22021793; PMCID: PMC3201768

[24] Toth AB, Shum AK, Prakriya M. Regulation of neurogenesis by calcium signaling. Cell Calcium. 2016;**59**(2-3):124-134. DOI: 10.1016/j.ceca.2016.02.011. PubMed PMID: 27020657; PMCID: PMC5228525

[25] Bezprozvanny I. Calcium signaling and neurodegenerative diseases. Trends in Molecular Medicine. 2009;**15**(3):89-100. DOI: 10.1016/j.molmed.2009.01.001. PubMed PMID: 19230774; PMCID: PMC3226745

[26] Perfettini JL, Roumier T, Kroemer G. Mitochondrial fusion and fission in the control of apoptosis. Trends in Cell Biology. 2005;**15**(4):179-183. Epub 2005/04/09. DOI: 10.1016/j.tcb.2005.02.005. PubMed PMID: 15817372. S0962-8924(05)00049-8 [pii]

[27] Youle RJ, Karbowski M. Mitochondrial fission in apoptosis. Nature reviews Molecular cell biology. 2005;**6**(8):657-663. Epub 2005/07/19. DOI: nrm1697 [pii]10.1038/nrm1697. PubMed PMID: 16025099

[28] Batlevi Y, La Spada AR. Mitochondrial autophagy in neural function, neurodegenerative disease, neuron cell death, and aging. Neurobiology of Disease. 2011;**43**(1):46-51. Epub 2010/10/05. DOI: 10.1016/j.nbd.2010.09.009. PubMed PMID: 20887789; PMCID: 3096708

[29] Rambold AS, Lippincott-Schwartz J. Mechanisms of mitochondria and autophagy crosstalk. Cell Cycle. 2011;**10**(23):4032-4038. Epub 2011/11/22. DOI: 10.4161/cc.10.23.18384. PubMed PMID: 22101267; PMCID: 3272286

[30] Benard G, Bellance N, James D, Parrone P, Fernandez H, Letellier T, Rossignol R. Mitochondrial bioenergetics and structural network organization. Journal of Cell Science. 2007;**120**(Pt 5):838-848. Epub 2007/02/15. DOI: 10.1242/jcs.03381. PubMed PMID: 17298981

[31] Grohm J, Kim SW, Mamrak U, Tobaben S, Cassidy-Stone A, Nunnari J, Plesnila N, Culmsee C. Inhibition of Drp1 provides neuroprotection in vitro and in vivo. Cell Death and Differentiation. 2012;**19**(9):1446-1458. Epub 2012/03/06. DOI: 10.1038/cdd.2012.18. PubMed PMID: 22388349; PMCID: 3422469

[32] Ong SB, Subrayan S, Lim SY, Yellon DM, Davidson SM, Hausenloy DJ. Inhibiting mitochondrial fission protects the heart against ischemia/reperfusion injury. Circulation. 2010;**121**(18):2012-2022. DOI: 10.1161/CIRCULATIONAHA.109.906610 Epub 2010/04/28. PubMed PMID: 20421521 CIRCULATIONAHA.109.906610 [pii]

[33] Boscolo A, Milanovic D, Starr JA, Sanchez V, Oklopcic A, Moy L, Ori CC, Erisir A, Jevtovic-Todorovic V. Early exposure to general anesthesia disturbs mitochondrial fission and fusion in the developing rat brain. Anesthesiology. 2013;**118**(5):1086-1097. DOI: 10.1097/ALN.0b013e318289bc9b. Epub 2013/02/16. PubMed PMID: 23411726

[34] Bartel DP. MicroRNAs: Genomics, biogenesis, mechanism, and function. Cell. 2004; **116**(2):281-297. PubMed PMID: 14744438

[35] Shukla GC, Singh J, Barik S. MicroRNAs: Processing, Maturation, Target Recognition and Regulatory Functions. Mol Cell Pharmacol. 2011;**3**(3):83-92. PubMed PMID: 22468167; PMCID: PMC3315687

[36] Zhang LF, Jiang S, Liu MF. MicroRNA regulation and analytical methods in cancer cell metabolism. Cellular and Molecular Life Sciences. 2017. DOI: 10.1007/s00018-017-2508-y. PubMed PMID: 28321489

[37] Twaroski DM, Yan Y, Olson JM, Bosnjak ZJ, Bai X. Down-regulation of microRNA-21 is involved in the propofol-induced neurotoxicity observed in human stem cell-derived neurons. Anesthesiology. 2014;**121**(4):786-800. DOI: 10.1097/ALN.0000000000000345. PubMed PMID: 24950164; PMCID: PMC4174986

[38] Bosnjak ZJ, Yan Y, Canfield S, Muravyeva MY, Kikuchi C, Wells CW, Corbett JA, Bai X. Ketamine induces toxicity in human neurons differentiated from embryonic stem cells via mitochondrial apoptosis pathway. Curr Drug Saf. 2012;**7**(2):106-119. PubMed PMID: 22873495; PMCID: PMC3684944

[39] Liu F, Paule MG, Ali S, Wang C. Ketamine-induced neurotoxicity and changes in gene expression in the developing rat brain. Current Neuropharmacology. 2011;**9**(1):256-261. DOI: 10.2174/157015911795017155. PubMed PMID: 21886601; PMCID: PMC3137194

[40] Tait SW, Green DR. Mitochondria and cell signalling. Journal of Cell Science. 2012;**125**(Pt 4): 807-815. DOI: 10.1242/jcs.099234. PubMed PMID: 22448037; PMCID: PMC3311926

[41] Wang W, Wang R, Zhang Q, Mor G, Zhang H. Benzo(a)pyren-7,8-dihydrodiol-9,10-epoxide induces human trophoblast Swan 71 cell dysfunctions due to cell apoptosis through disorder of mitochondrial fission/fusion. Environmental Pollution. 2017;**233**:820-832. DOI: 10.1016/j.envpol.2017.11.022. PubMed PMID: 29144987

[42] Yu Y, Xu L, Qi L, Wang C, Xu N, Liu S, Li S, Tian H, Liu W, Xu Y, Li Z. ABT737 induces mitochondrial pathway apoptosis and mitophagy by regulating DRP1-dependent mitochondrial fission in human ovarian cancer cells. Biomedicine & Pharmacotherapy. 2017;**96**:22-29. DOI: 10.1016/j.biopha.2017.09.111. PubMed PMID: 28963947

[43] Li S, Zhao H, Wang Y, Shao Y, Li J, Liu J, Xing M. The inflammatory responses in Cu-mediated elemental imbalance is associated with mitochondrial fission and intrinsic

apoptosis in Gallus gallus heart. Chemosphere. 2017;**189**:489-497. DOI: 10.1016/j.chemosphere.2017.09.099. PubMed PMID: 28957766

[44] Cui J, Li Z, Zhuang S, Qi S, Li L, Zhou J, Zhang W, Zhao Y. Melatonin alleviates inflammation-induced apoptosis in human umbilical vein endothelial cells via suppression of Ca^{2+}-XO-ROS-Drp1-mitochondrial fission axis by activation of AMPK/SERCA2a pathway. Cell Stress & Chaperones. 2017. DOI: 10.1007/s12192-017-0841-6. PubMed PMID: 28889229

[45] Zhao G, Cao K, Xu C, Sun A, Lu W, Zheng Y, Li H, Hong G, Wu B, Qiu Q, Crosstalk LZ. Between mitochondrial fission and oxidative stress in Paraquat-induced apoptosis in mouse alveolar type II cells. International Journal of Biological Sciences. 2017;**13**(7):888-900. DOI: 10.7150/ijbs.18468. PubMed PMID: 28808421; PMCID: PMC5555106

[46] Gou H, Zhao M, Xu H, Yuan J, He W, Zhu M, Ding H, Yi L, Chen JCSFV. Induced mitochondrial fission and mitophagy to inhibit apoptosis. Oncotarget. 2017;**8**(24):39382-39400. DOI: 10.18632/oncotarget.17030. PubMed PMID: 28455958; PMCID: PMC5503620

[47] Budd SL, Tenneti L, Lishnak T, Lipton SA. Mitochondrial and extramitochondrial apoptotic signaling pathways in cerebrocortical neurons. Proceedings of the National Academy of Sciences of the United States of America. 2000;**97**(11):6161-6166. Epub 2000/05/17. DOI: 10.1073/pnas.100121097100121097 [pii]. PubMed PMID: 10811898; PMCID: 18575

[48] Braun S, Gaza N, Werdehausen R, Hermanns H, Bauer I, Durieux ME, Hollmann MW, Stevens MF. Ketamine induces apoptosis via the mitochondrial pathway in human lymphocytes and neuronal cells. British Journal of Anaesthesia. 2010;**105**(3):347-354. Epub 2010/07/28. DOI: aeq169 [pii]10.1093/bja/aeq169. PubMed PMID: 20659914

[49] Zhang Y, Dong Y, Wu X, Lu Y, Xu Z, Knapp A, Yue Y, Xu T, Xie Z. The mitochondrial pathway of anesthetic isoflurane-induced apoptosis. Journal of Biological Chemistry. 2010;**285**(6):4025-4037. Epub 2009/12/17. DOI: M109.065664 [pii] 10.1074/jbc.M109.065664. PubMed PMID: 20007710; PMCID: 2823544

[50] Takadera T, Ishida A, Ohyashiki T. Ketamine-induced apoptosis in cultured rat cortical neurons. Toxicology and Applied Pharmacology. 2006;**210**(1-2):100-107. Epub 2005/11/26. DOI: S0041-008X(05)00599-5 [pii]10.1016/j.taap.2005.10.005. PubMed PMID: 16307766

[51] Zou X, Patterson TA, Sadovova N, Twaddle NC, Doerge DR, Zhang X, Fu X, Hanig JP, Paule MG, Slikker W, Wang C. Potential neurotoxicity of ketamine in the developing rat brain. Toxicological Sciences. 2009;**108**(1):149-158. Epub 2009/01/08. DOI: kfn270 [pii]10.1093/toxsci/kfn270. PubMed PMID: 19126600; PMCID: 2721655

[52] Soriano SG, Liu Q, Li J, Liu JR, Han XH, Kanter JL, Bajic D, Ibla JC. Ketamine activates cell cycle signaling and apoptosis in the neonatal rat brain. Anesthesiology. 2010;**112**(5):1155-1163. Epub 2010/04/27. DOI: 10.1097/ALN.0b013e3181d3e0c200000542-201005000-00021 [pii]. PubMed PMID: 20418696

[53] Reddy PH. Role of mitochondria in neurodegenerative diseases: mitochondria as a therapeutic target in Alzheimer's disease. CNS Spectrums. 2009;**14**(8 Suppl 7):8-13; discussion 6-8. PubMed PMID: 19890241; PMCID: PMC3056539

[54] Twaroski DM, Yan Y, Zaja I, Clark E, Bosnjak ZJ, Bai X. Altered mitochondrial dynamics contributes to Propofol-induced cell death in human stem cell-derived neurons. Anesthesiology. 2015;**123**(5):1067-1083. DOI: 10.1097/ALN.0000000000000857. PubMed PMID: 26352374; PMCID: PMC4632973

[55] Sathyan P, Golden HB, Miranda RC. Competing interactions between micro-RNAs determine neural progenitor survival and proliferation after ethanol exposure: Evidence from an ex vivo model of the fetal cerebral cortical neuroepithelium. The Journal of Neuroscience. 2007;**27**(32):8546-8557. DOI: 10.1523/JNEUROSCI.1269-07.2007. PubMed PMID: 17687032; PMCID: PMC2915840

IntechOpen